Pergamon

Cement and Concrete Research 32 (2002) 1377–1382

CEMENT AND CONCRETE RESEARCH

# Autoclave properties of kirschsteinite-based steel slag

Guangren Qian[a,*], Darren Delai Sun[a], Joo Hwa Tay[a], Zhenyu Lai[b], Guangliang Xu[b]

[a]*Environmental Engineering Research Centre, School of Civil Structural and Engineering, Nanyang Technological University, Singapore 639789, Singapore*
[b]*Southwest University of Science and Technology, Mianyang 621002, Sichuan, People's Republic of China*

Received 15 October 2001; accepted 11 March 2002

## Abstract

The kirschsteinite-based steel slag is one kind of low-alkalinity steel slag. This steel slag hardly behaves as any hydraulicity. In this paper, the hydrothermal products and binding properties of this slag, after being subjected to autoclave treatments, were evaluated. The results show that a hydrothermal autoclave reaction could modify the binding behaviours of kirschsteinite-based steel slag. The main hydrothermal product of pure kirschsteinite-based steel slag was Fe-hydrogarnet, which exhibited poor binding strength. However, the system of quartz–kirschsteinite steel slag appeared to have excellent binding properties due to autoclave treatment, in which the kirschsteinite phase was hydrothermally changed into Fe-substituted tobermorite. Meanwhile, Fe-substituted tobermorite phase was still stable relative to xonotlite over 345 °C.

*Keywords:* Kirschsteinite-based steel slag; Autoclave binding properties; Hydrothermal products

## 1. Introduction

Steel slag includes basic oxygen furnace (BOF) and electric arc furnace (EAF) slags. Most of BOF slags have similar chemical compositions and mineral phases as Portland cement clinker. In the recent decades, these BOF slags have been successfully used as supplementary materials of Portland cement and raw materials of making brick. Compared with BOF slag, most of EAF steel slags are with less CaO in chemical compositions. The dominant minerals of EAF steel slag can be classified into dicalcium silicate ($C_2S$), merwinite ($C_3MS_2$) or kirschsteinite (CFS), depending on the alkalinity ($CaO/(SiO_2+P_2O_5)$) of steel slag, of which the alkalinity of kirschsteinite is the lowest. When reacted with water at normal temperature, these EAF steel slags can hardly hydrate so that only poor binding properties, and even no hydraulicity, are expected. Here, we refer to these EAF steel slags as low-alkalinity steel slag.

As viewed from the mineral phases, the alkalinity of low-alkalinity steel slag is basically similar to that of traditional oilwell cement clinker or geowell binding materials. The excellent binding properties of oilwell and geowell binding materials result from hydrothermal reaction, which is self-produced under high-temperature and high-pressure environment [1]. Вохженов [2] reported that the transformation of olivine mineral into cementitious magnesium silicate hydrate in the metamorphic rock was due to a geologically hydrothermal metamorphous role. Meanwhile, the hydrothermal products of inert minerals such as $\gamma$-$C_2S$, merwinite ($3CaO \cdot MgO \cdot 2SiO_2$) and akermanite ($2CaO \cdot MgO \cdot 2SiO_2$) have been reported by many researches [3–6]. These inert minerals would form potential high-temperature binding products: tobermorite, gyrolite, truscottite and xonotlite. Based on the above consideration, low-alkalinity steel slag-based oilwell and geowell binding materials have been explored in our laboratory. In this paper, hydrothermal products and binding behaviour produced by kirschseinite-based steel slag are present.

## 2. Experimental

### 2.1. Steel slag samples

EAF steel slag was from Natsteel (Singapore, Singapore). After analyzing its chemical compositions, the

---

* Corresponding author. Permanent address: School of Materials Science and Engineering, Southwest University of Science and Technology, Mianyang 621002, Sichuan, People's Republic of China.

*E-mail addresses*: qgr@swust.edu.cn, cgrqian@ntu.edu.sg (G. Qian).

0008-8846/02/$ – see front matter © 2002 Elsevier Science Ltd. All rights reserved.
PII: S0008-8846(02)00790-1

mineral phases were characterized by polarized light microscopy and X-ray diffraction.

### 2.2. Autoclave reaction

Steel slag particles were ground to fineness at 450–500 $m^2$/kg. Quartz powder, which contains more than 98% $SiO_2$ and has a specific surface of 350 $m^2$/kg, was used. Two autoclave samples were prepared. One was pure EAF steel slag powder; the other was a mixture of steel slag and quartz, in which the $CaO/SiO_2$ mole ratio was adjusted around 0.8.

The pastes of these mixtures were cast into the cubic moulds with a size of 20 × 20 × 20 mm. The W/C ratio of the paste was 0.2. After being cured in humidity for 24 h at ambient temperature, hardened cubic blocks were removed from the moulds and then steamed at 100 °C for 4 h. Finally, these steamed cubic blocks were autoclaved, respectively, at 2 MPa (217 °C) and 15 MPa (345 °C) at different times. The compressive strength tests of autoclaved cubic blocks were also carried out.

### 2.3. Analysis of hydration products

All samples that were autoclaved for various times were examined by X-ray powder diffraction, scanning electron microscopy and DSC to detect the reaction phases formed.

## 3. Results and discussions

### 3.1. Mineral phases of kirschsteinite-based steel slag

The chemical compositions of EAF steel slag selected for this test are listed in Table 1. The alkalinity of this steel slag is 1.16, far lower than common BOF slag. It contains about 30% FeO and 9% MgO. The mineral phases of this steel slag were detected by XRD. As illustrated in Fig. 1, most of the main peaks such as at 5.55, 2.95 and 2.61 Å were well matched with that of kirschsteinite phase, showing that kirschsteinite was a dominant phase of this slag. Additionally, some main peaks at 2.48, 2.143 and 1.48 Å were due to the existence of the wustite phase. Theoretically, the main reflection of pure wustite phase stands at 2.153 Å. EXD results detected that this wustite phase contains 21% MgO, 6% CaO and 4% MnO besides 69% FeO. It suggests that this wustite phase is one kind of RO phase, referred to as Mg-wustite [7]. The shift of the *d* value, from 2.153 to 2.143 Å, could be attributed to the incorporation of Mg ion in the wustite lattice. Under polarized microscopy (Fig. 2), the kirschsteinite phase exists in the form of grains, colourless and transparent; Mg-wustite phases, seal brown and irregular round in shape, are filled between kirschsteinite phases. By semiquantitative analysis, this EAF steel slag contains 50–60% kirschsteinite and 40–50% Mg-wustite phases. Therefore, it is a kirschsteinite-based steel slag.

Table 1
Chemical compositions and mineral phases of sample

| Chemical compositions (wt.%) | | | | $CaO/(SiO_2+P_2O_5)$ | Mineral phases |
|---|---|---|---|---|---|
| CaO | 22.48 | $Fe_2O_3$ | 8.49 | 1.14 | CFS RO (Mg-wustite) |
| $SiO_2$ | 19.38 | FeO | 30.54 | | |
| $Al_2O_3$ | 5.27 | MnO | 1.10 | | |
| MgO | 9.51 | F-CaO | N.D. | | |
| $P_2O_5$ | 0.35 | | | | |

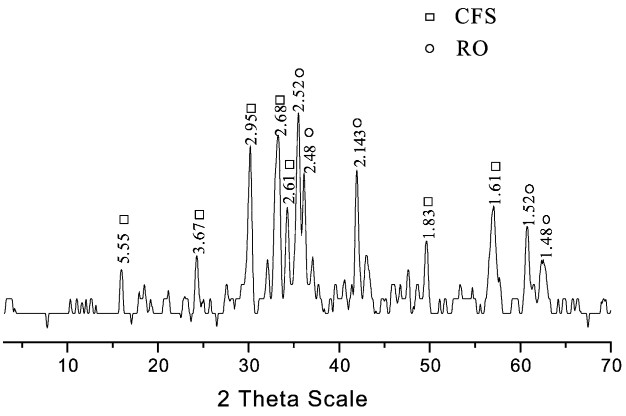

Fig. 1. XRD pattern of pure steel slag.

### 3.2. Autoclave binding properties of kirschsteinite-based steel slag

As one of olivine group minerals, kirschsteinite phase is a typical nesosilicates. At ambient temperature, kirschsteinite-based steel slag hardly showed any hydaulicity. When steamed at 100 °C for 4 h, it began to slightly harden but its compressive strength was difficult to detect accurately.

Hydrothermal treatment at autoclave condition provided this kirschsteinite-based steel slag with binding properties. Fig. 3a shows the compressive strengths of pure steel slag.

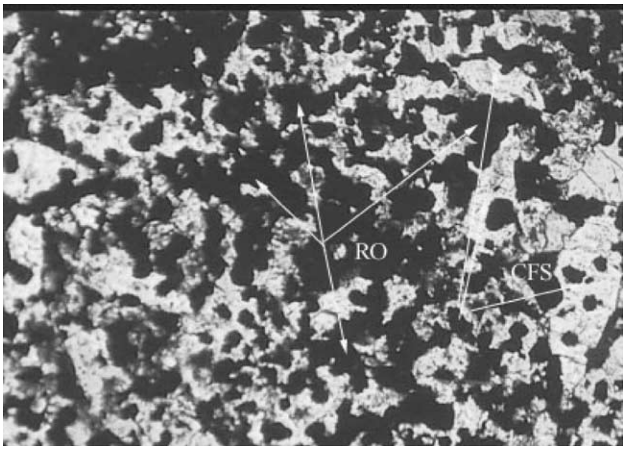

Fig. 2. Microstructure of pure steel slag (polarized microscopy, × 50).

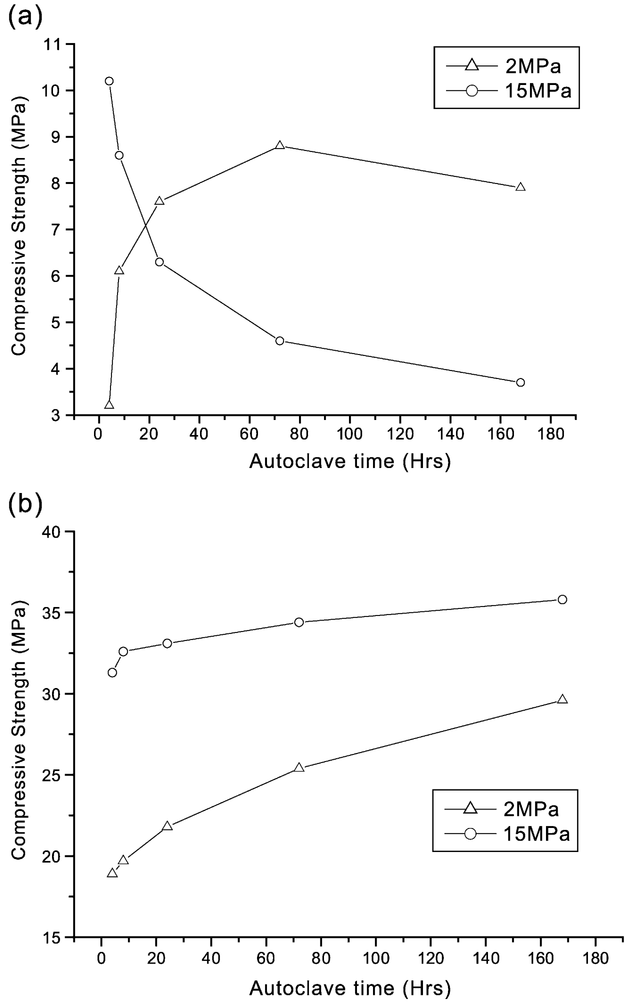

Fig. 3. Autoclave compressive strength of kirschsteinite-based steel slag. (a) Pure steel slag. (b) Steel slag–quartz.

When pure steel slag was autoclaved at 2 MPa, its compressive strength was 3.2 MPa for 4 h. It increased with the treatment time and reached 7.9 MPa for 168 h. When the autoclave temperature was enhanced to 15 MPa (345 °C), the compressive strength of sample was increased to 10.2 MPa for 4 h. But at this temperature, it did not continue to rise with prolonged autoclave times but instead slightly dropped, even lower than that at 2 MPa after treatment for 24 h.

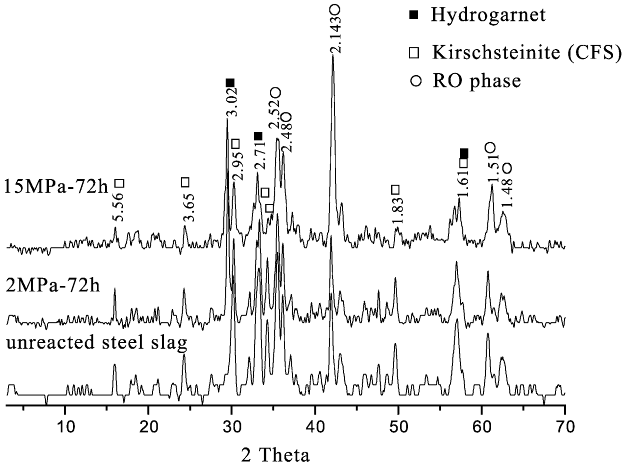

Fig. 4. XRD patterns of autoclave product for pure steel slag.

The autoclave strengths of steel slag–quartz system were plotted in Fig. 3b. The autoclave binding properties of kirschsteinite slag were highly improved due to the addition of siliceous substance. The compressive strength at 2 MPa for 4 h reached 18.9 MPa, five times higher than that of pure steel slag. Meanwhile, it rapidly increased with time and went up to 29.6 MPa for 168 h. The temperature has a rather positive role on the strength development of steel slag–quartz system. Only autoclaved at 15 MPa for 4 h, the strength of blend sample had reached up to 31.3 MPa, 66% more than that at 2 MPa. When the autoclave treating went on, however, the strengths of the blend samples only slightly increased and the maximum strength of 35.1 MPa was detected while being treated for 168 h.

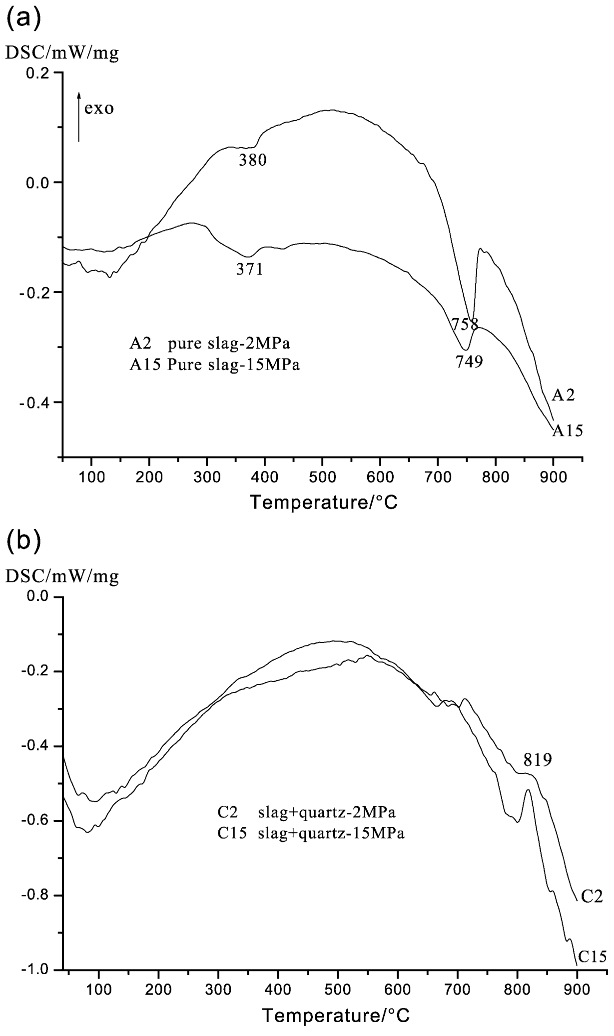

Fig. 5. DSC patterns of autoclave product for different steel slag samples. (a) Pure steel slag. (b) Steel slag–quartz.

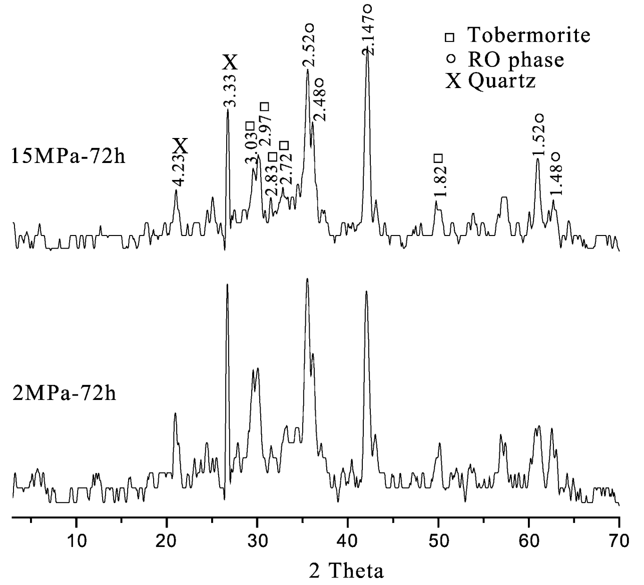

Fig. 6. XRD patterns of autoclave product for steel slag samples added with quartz.

### 3.3. Hydrothermal product properties of kirschsteinite-based steel slag

The kirschsteinite-based steel slag belongs to the CaO–$SiO_2$–$Fe_2O_3$–MgO system. Compared with olivine mineral, the kirschsteinite phase is rich in iron and poor in Mg, although it also belongs to nesosilicates. It had been noticed that the olivine phase is changed into the cementitious serpentine phase by a geological, hydrothermal metamorphous process. Unlike olivine, however, the kirschsteinite phase did not transform into serpentine during the process of hydrothermal reaction. The XRD patterns of hydrothermal products for pure kirschsteinite slag are shown in Fig. 4. It can be seen that the main reflections of kirschsteinite phase at 5.56, 2.95 and 2.61 Å dropped a lot after being autoclaved at 2 MPa for 72 h. Instead, a new phase corresponding to the main reflections at 3.02, 2.71 and 1.61 Å occurred. This new phase was identified as hydrogarnet. When treated at 15 MPa for 72 h, this hydrogarnet phase also existed stably and a part of kirschsteinite phase still remained in existence. It suggests that kirschsteinite is an unstable phase in the hydrothermal process, in which it can be changed into hydrogarnet phase. However, the kinetic rate of this transformation was not so quick as other nesosilicates such as the merwinite phase [5]. Additionally, the hydrothermal reaction degree of Mg-wustite phase was difficult to be estimated by XRD results as it was scarcely changed after autoclave treatment. As seen in Fig. 4, its main reflection at 2.143 Å was still kept strong even at 15 MPa for 72 h. The above reaction process was further confirmed by DSC patterns in Fig. 5a. The strong endothermal peak at 758 °C is due to the decomposition of hydrogarnet phase. Meanwhile, a poor endothermal peak at 370–380 °C can be observed whatever the temperature is, which is ascribed to the decomposition of the brucite phase. Apparently, this brucite phase was formed by the hydrothermal reaction of Mg-wustite phase. It reveals that the Mg-wustite phase also has a potential to participate in a hydrothermal reaction to form brucite.

The excellent autoclave binding properties of steel slag–quartz system were controlled by their hydrothermal products. As shown in Fig. 6, the hydrothermal products of this system were quite different from those of pure steel slag. Firstly, the hydrogarnet phase did not occur in this system. With kirschsteinite phase decreased gradually, some new main reflections at 3.03, 2.97, 2.83 and 1.82 Å became strong except that the peak at 11 Å was lacking. These new peaks are deduced to tobermorite phase. Moreover, this tobermorite phase could also be well distinguished even if treated at 2 MPa. The DSC results in Fig. 5b support the presence of this tobermorite phase. It gave an exothermal peak at 819 °C in DSC patterns. The exothermal peak

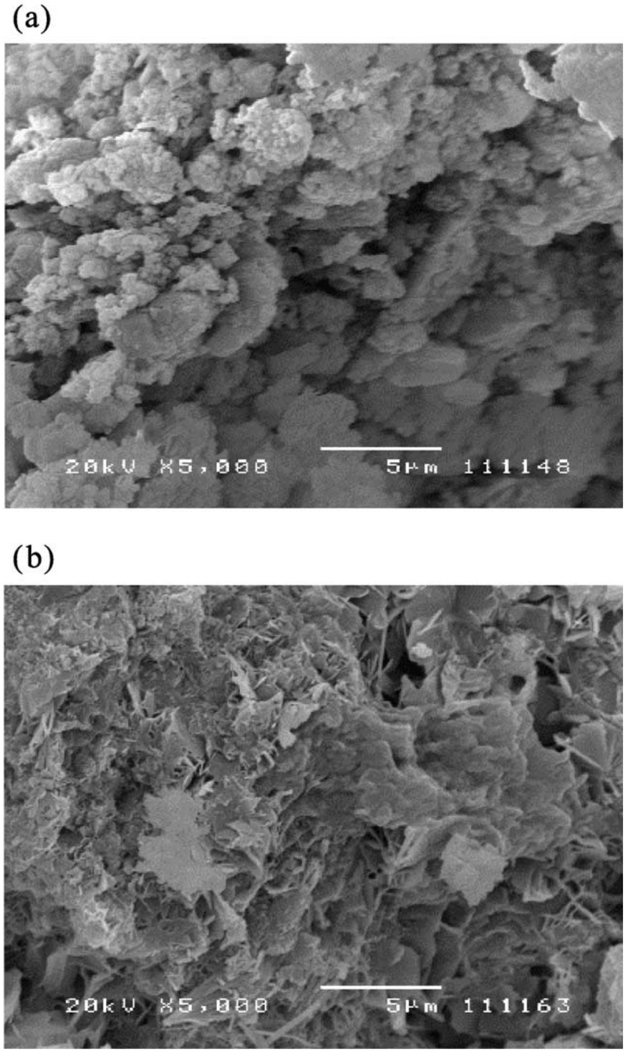

Fig. 7. SEM morphologies of hydrothermal products for steel slag samples after being autoclaved for 72 h at 15 MPa. (a) Pure steel slag system. (b) Steel slag–quartz system.

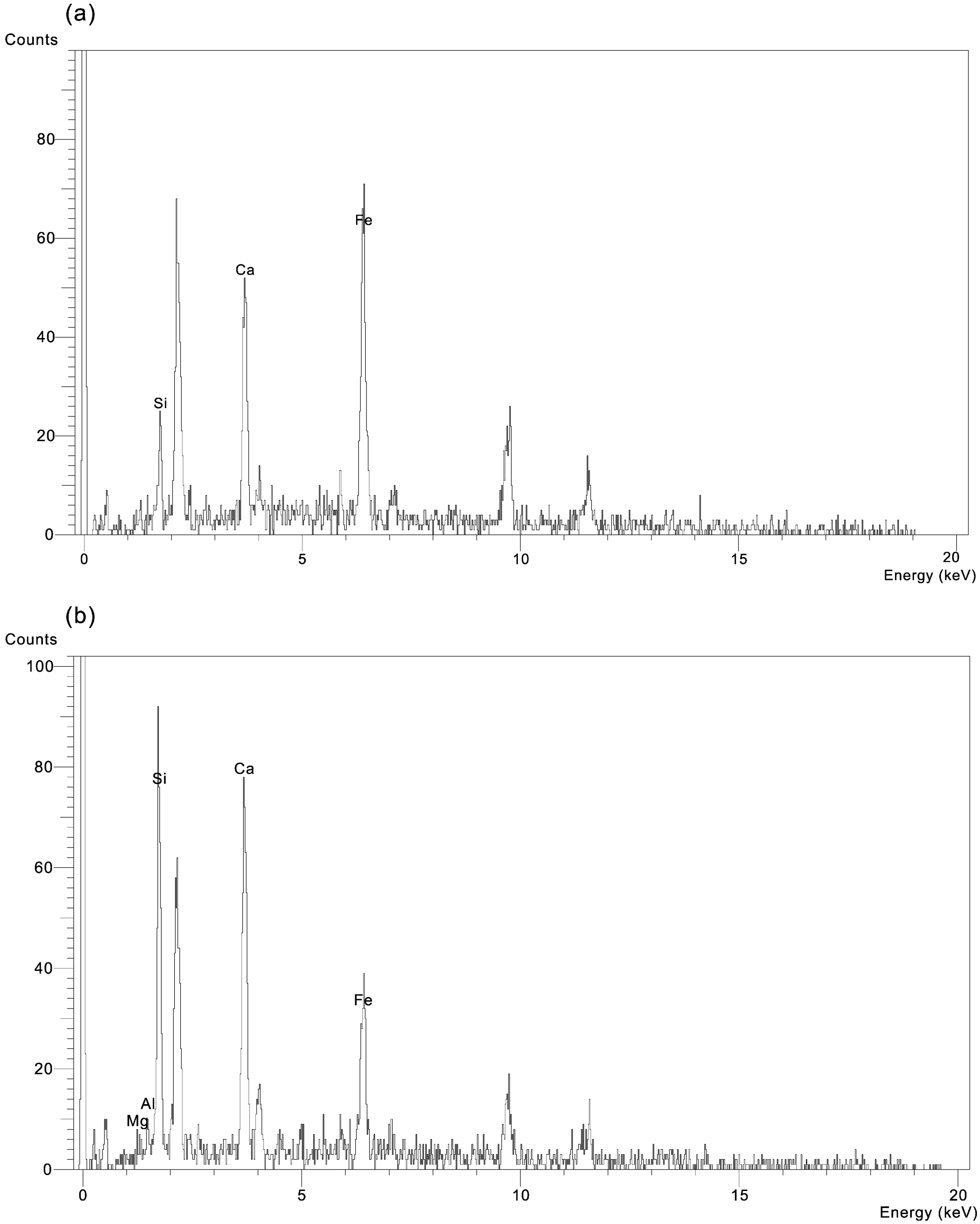

Fig. 8. EDX pattern of hydrothermal products. (a) Hydrogarnet. (b) Tobermorite.

formed at 2 MPa appeared as a poor hump and became bigger and sharper at 15 MPa. Therefore, it can be concluded that kirschsteinite would react with silica to form a tobermorite phase under hydrothermal conditions.

Secondly, Speakman [8] established that the tobermorite phase is unstable with respect to xonotlite above 140 °C. However, the substitution of Al in the tobermorite lattice appears to extend the range of stability of tobermorite. Scheetz and Roy [9] found Al-substituted tobermorite in hydrothermal cements at 300 °C. As described above, the dominant phase in the kirschsteinite–quartz system was still tobermorite, rather than xonotlite, when the autoclave treatment was enhanced to 345 °C. It suggests that the tobermorite phase is still stable at 345 °C.

Thirdly, the endothermal peak of the brucite phase in DSC patterns did not occur when steel slag was reacted with quartz. Qian et al. [10,11] established that $Mg^{2+}$ would be preferentially incorporated into calcium silicate hydrates such as tobermorite, gyrolite and xonotlite. The following EDX results have proven this.

The microstructures of autoclave products were observed by SEM and the distributions of elements in the products were detected by EDX. As shown in Fig. 7a, most of the hydrothermal products for pure steel slag were in irregular spheric and cubic grains, which are related to hydrogarnet morphology. There were a lot of micropores between irregular grains so that they were not well bound together. The EDX result in Fig. 8a indicates that there existed 20–30 wt.% Fe and few Mg in the hydrogarnet product besides Ca and Si atoms. According to this, it can be deduced that the hydrogarnet formed hydrothermally by the kirschsteinite phase is Fe-hydrogarnet.

The tobermorite phases in steel slag–quartz system occurred in the form of crinkled foils and thin platelet-like morphology (Fig. 7b). No other sphere or cubic grains were observed. It was these well interlocked semicrystalline products that provided materials with excellent binding properties. The EDX result in Fig. 8b reveals that 10–15 wt.% Fe and few Mg were incorporated in the tobermorite phase. Hereby, it can be inferred that it was the incorporation of Fe that inhibited the Fe-substituted tobermorite phase from transforming into xonotlite phase so that Fe-substituted tobermorite phase would still exist stably over 345 °C.

Based on the above discussion, the hydrothermal reaction of kirschsteinite phase can be expressed as:

$$\mathrm{CaO \cdot FeO \cdot SiO_2(CFS)} \xrightarrow{\text{hydrothermal reaction}} \mathrm{Ca_3Fe_2} \times \mathrm{(SO_4)_{3-x}(OH)_{4-x}} \quad \mathrm{Fe} - \text{hydrogarnet}$$

$$\mathrm{CaO \cdot FeO \cdot SiO_2(CFS)} + \mathrm{SiO_2} \xrightarrow{\text{hydrothermal reaction}} \mathrm{5CaO \cdot 6Si(Fe)O_2 \cdot 4H_2O} \quad \mathrm{Fe} - \text{substituted Tob.}$$

## 4. Conclusions

1. A hydrothermally autoclaved reaction can provide kirschsteinite-based steel slag with excellent binding properties.
2. The main hydrothermal product of pure kirschsteinite-based steel slag was Fe-hydrogarnet. The kirschsteinite phase would be hydrothermally changed into Fe-substituted tobermorite in the system of quartz–kirschsteinite-based steel slag.
3. The Fe-substituted tobermorite phase was still stable relative to xonotlite over 345 °C.

## Acknowledgments

The authors are grateful to The National Natural Science Fund of China and The National Science and Technology Board of Singapore for financial support on this project. The series number of this project is 59674034.

## References

[1] H.F.W. Taylor, Cement Chemistry, second ed., Thomas Telford, England, 1997.

[2] П.И. Вохженов, Technique of Autoclave Materials, Translated by Civil Engineering Publishing House, China, Beijing, 1978.

[3] G.L. Kalousek, E.B. Nelson, Hydrothermal reactions of dicalcium silicate and silica, Cem. Concr. Res. 8 (3) (1978) 283–289.

[4] J. Jernejcic, I. Jelnic, Properties of autoclaved and thermally treated moulds made from gamma-$C_2S$ and quartz at C/S ratios 0.5 to 1.5, Cem. Concr. Res. 4 (1) (1974) 23–32.

[5] G.R. Qian, A.M. Li, G.L. Xu, H.Y. Li, Hydrothemal products of the $C_3MS_2$–$C_{12}A_7$–MgO system, Cem. Concr. Res. 27 (12) (1997) 1791–1797.

[6] A. Kiyoshi, T. Jun, D. Masaki, H.L. Kyung, Reaction rate of akermanite, $Ca_2MgSi_2O_7$ under hydrothermal condition, Gypsum Lime 202 (1) (1986) 22–27.

[7] G.R. Qian, D.D. Sun, J.W. Tay, Hydrothermal reaction and autoclave stability of Mg-bearing RO phase in Steel Slag, Trans. Br. Ceram. (2002) (in press).

[8] K. Speakman, The stability of tobermorite in the system CaO–$SiO_2$–$H_2O$ at elevated temperature and pressures, Mineral. Mag. 36 (6) (1968) 1090–1103.

[9] B.E. Scheetz, D.M. Roy, Preliminary Survey of the Stability of Silica-Rich Cementitious Mortar, 8L-22 and 84-12 Tuff, LA 11222-MS, 00-70, Los Alamos National Laboratory, Los Alamos, NM, 1989.

[10] G.R. Qian, G.L. Xu, H.Y. Li, A.M. Li, The effect of autoclave temperature on the expansion and hydrothermal products of high-MgO blended cements, Cem. Concr. Res. 28 (1) (1998) 1–6.

[11] G.R. Qian, G.L. Xu, H.Y. Li, A.M. Li, Mg-xonotlite and its coexisting phases, Cem. Concr. Res. 27 (3) (1997) 315–320.